Voltage modulates halothane-triggered Ca^{2+} release in malignant hyperthermia-susceptible muscle

Alberto Zullo,[1,4,5]* Martin Textor,[1]* Philipp Elischer,[1] Stefan Mall,[1] Andreas Alt,[2] Werner Klingler,[3,6] and Werner Melzer[1]

[1]Institute of Applied Physiology and [2]Institute of Legal Medicine, Ulm University, Ulm, Germany
[3]Department of Neuroanaesthesiology, Ulm University, Günzburg, Germany
[4]CEINGE - Biotecnologie Avanzate, Napoli, Italy
[5]Department of Sciences and Technologies, University of Sannio, Benevento, Italy
[6]Queensland University of Technology, Brisbane, Australia

Malignant hyperthermia (MH) is a fatal hypermetabolic state that may occur during general anesthesia in susceptible individuals. It is often caused by mutations in the ryanodine receptor RyR1 that favor drug-induced release of Ca^{2+} from the sarcoplasmic reticulum. Here, knowing that membrane depolarization triggers Ca^{2+} release in normal muscle function, we study the cross-influence of membrane potential and anesthetic drugs on Ca^{2+} release. We used short single muscle fibers of knock-in mice heterozygous for the RyR1 mutation Y524S combined with microfluorimetry to measure intracellular Ca^{2+} signals. Halothane, a volatile anesthetic used in contracture testing for MH susceptibility, was equilibrated with the solution superfusing the cells by means of a vaporizer system. In the range 0.2 to 3%, the drug causes significantly larger elevations of free myoplasmic [Ca^{2+}] in mutant (YS) compared with wild-type (WT) fibers. Action potential–induced Ca^{2+} signals exhibit a slowing of their time course of relaxation that can be attributed to a component of delayed Ca^{2+} release turnoff. In further experiments, we applied halothane to single fibers that were voltage-clamped using two intracellular microelectrodes and studied the effect of small (10-mV) deviations from the holding potential (−80 mV). Untreated WT fibers show essentially no changes in [Ca^{2+}], whereas the Ca^{2+} level of YS fibers increases and decreases on depolarization and hyperpolarization, respectively. The drug causes a significant enhancement of this response. Depolarizing pulses reveal a substantial negative shift in the voltage dependence of activation of Ca^{2+} release. This behavior likely results from the allosteric coupling between RyR1 and its transverse tubular voltage sensor. We conclude that the binding of halothane to RyR1 alters the voltage dependence of Ca^{2+} release in MH-susceptible muscle fibers such that the resting membrane potential becomes a decisive factor for the efficiency of the drug to trigger Ca^{2+} release.

INTRODUCTION

Halogenated gaseous drugs are extensively used for inducing reversible loss of consciousness in general anesthesia. These drugs are thought to perform their function through weak interactions with specific protein targets such as GABA-A and NMDA receptors in brain regions involved in the control of sleep and arousal (Franks, 2008).

A possible devastating side effect of volatile anesthetics is the induction of malignant hyperthermia (MH) in genetically predisposed individuals. MH is a hypermetabolic crisis resulting from an increase in the cytoplasmic Ca^{2+} concentration in skeletal muscle leading to muscle rigidity, hyperthermia, acidosis, tachycardia, hyperkalemia, and rhabdomyolysis (Rosenberg et al., 2015). It originates from a drug-induced leakiness of the SR, mostly caused by mutations in the Ca^{2+} release channel (ryanodine receptor RyR1; Hwang et al., 2012; Guerrero-Hernández et al., 2014). In recent years, several of these human mutations have been introduced into the mouse genome (Chelu et al., 2006; Yang et al., 2006), providing excellent murine models to study the functional implications on the organismic and cellular level.

A functional hallmark of MH susceptibility is a significantly higher sensitivity to a variety of contraction-inducing drugs (Hopkins, 2011). This is the basis of standardized diagnostic tests (in vitro contracture tests [IVCTs]) that use force recording on muscle biopsies and use caffeine and halothane as triggering drugs (Larach, 1989; Rosenberg et al., 2002; Hopkins et al., 2015). The animal model used in the present study is based on human RyR1 mutation Y522S (Y524S in the mouse genome) and shows strong and lethal MH-like episodes caused by either application of volatile anesthetics or elevated ambient temperature (Chelu et al., 2006).

RyR1 is located in the membrane of the terminal cisternae of the SR and is in mechanical contact with the

*A. Zullo and M. Textor contributed equally to this paper.
Correspondence to Werner Melzer: werner.melzer@uni-ulm.de

The Rockefeller University Press
J. Gen. Physiol. 2018 Vol. 150 No. 1 111–125
https://doi.org/10.1085/jgp.201711864

dihydropyridine receptor (DHPR; L-type Ca^{2+} channel, CaV1.1) of the adjacent transverse tubular membrane (Franzini-Armstrong and Protasi, 1997; Van Petegem, 2015). The DHPR serves as a sensor of the cell membrane potential. Action potentials initiated at the postsynaptic face of the neuromuscular junction spread into the transverse tubular system and cause rapid release of Ca^{2+} from the SR, which activates contraction (Lanner et al., 2010; Hernández-Ochoa et al., 2016). The Ca^{2+} release results from the voltage-induced conformational signal transmission from the DHPR to the RyR1 and does not require any entry of Ca^{2+} from the outside through the L-type Ca^{2+} channel (Armstrong et al., 1972; Spiecker et al., 1979; Melzer et al., 1995; Dayal et al., 2017), contrary to the situation in heart muscle (Eisner et al., 2017).

Because RyR1, the central protein in excitation-contraction coupling (ECC), is voltage-activated via the DHPR, MH mutations in RyR1 can be expected to affect depolarization-induced Ca^{2+} release. That this is indeed the case has been demonstrated on various occasions. The first hint was the demonstration by Gallant and co-workers that external potassium-induced contraction exhibited a lower threshold in muscle of MH-susceptible (MHS) pigs compared with controls (Gallant and Donaldson, 1989; Gallant and Lentz, 1992). In agreement with this observation, our group demonstrated that the voltage threshold for Ca^{2+} release in MHS muscle cells was lower than in normal myocytes (Dietze et al., 2000; Andronache et al., 2009). Given the higher voltage sensitivity of the ECC system in muscle cells with mutant RyR1, it can be speculated, but has not yet been demonstrated, that halogenated anesthetics may further lower the threshold of voltage-activated Ca^{2+} release.

The basis of our study, therefore, is the hypothesis that MH-inducing gaseous drugs, when acting directly on the RyR1, will alter characteristics of voltage-activated Ca^{2+} release. These could show up as alterations of the time course and amplitude of voltage-triggered Ca^{2+} release and as a change in its voltage dependence.

We pursued this question by recording Ca^{2+} signals in single isolated muscle fibers of WT and MH-susceptible mice and applying the volatile anesthetic drug halothane. The membrane potential was altered by eliciting action potentials and using a voltage clamp method.

MATERIALS AND METHODS

Preparation

Male heterozygous WT/Y524S mice (Chelu et al., 2006) and age-matched homozygous WT littermates were used for the experiments. For simplicity, the genotypes will be referred to as YS (mutant) and WT, respectively. The animals were bred in the specific pathogen–free facility of the Animal Research Center of Ulm University.

All experimental procedures performed on mice were in accordance with German animal protection laws, approved by the local animal welfare committee, and conducted under the project license O.47 of the Institutional Animal Care and Use Committee of Ulm University (Tierforschungszentrum, Universität Ulm) with approval by the regional administrative authority (Regierungspräsidium Tübingen). Adult mice were killed by CO_2 application and rapid cervical dislocation. Interosseous muscles were dissected from the hind limbs in Ringer's solution. Single muscle fibers were enzymatically dissociated in Ringer's solution containing 2 mg/ml collagenase (Liu et al., 1997; Ursu et al., 2005).

Experimental solutions

Ringer's solution for extracellular stimulation experiments was (mM) 145 NaCl, 5 KCl, 1 $MgCl_2$, 2.5 $CaCl_2$, 10 HEPES, 0.1 *N*-benzyl-p-toluene sulfonamide (BTS), and 10 glucose, pH 7.4. External (bathing) solution for voltage clamp experiments was (mM) 130 TEA-OH, 130 HCH_3SO_3, 1 $MgCl_2$, 2.5 $CaCl_2$, 5 4-aminopyridine, 10 HEPES, 0.001 tetrodotoxin, 10 glucose, and 0.05 BTS, pH 7.4.

Electrophysiology and calcium recording

Cells were loaded with 5 µM fura-2-AM for 45 min. Remaining external dye was washed out with the experimental solution, and the cells were incubated for 30 min to allow for full intracellular cleavage of the acetoxymethyl ester. The myosin II blocker BTS was added to suppress muscle contraction.

Measurements of action potential–triggered fura-2 Ca^{2+} signals were performed as described (Braubach et al., 2014) using an inverted fluorescence microscope (Axiovert 100; Zeiss) equipped with a photomultiplier tube and extracellular stimulation system. Rectangular current pulses (0.5-ms duration) were applied through two stainless steel electrodes immersed in the bath solution close to the cell. Screening for responsive cells was performed using sequential pulses of different voltage (6, −7, 8, and −9 V). Then, pulses of equal size but opposite sign, spaced 500 ms apart, were applied, and their amplitudes were gradually increased. Measurements were confined to cells that produced equal all-or-none reactions to both the positive and the negative stimuli. The final pulse voltage for further measurements was set to 1 V above the excitation threshold. Fluorescence was excited consecutively with UV light of 360 nm (near isosbestic wavelength) and 380 nm (bandwidth 10 and 15 nm, respectively). Fibers were stimulated during the 380-nm irradiation interval.

Fluorescence ratio signals R = F380/F360 (for 380 and 360 nm excitation, respectively) were calculated and converted to free Ca^{2+} concentration ($[Ca^{2+}]$), including temporal deconvolution (Carroll et al., 1995), using dissociation constant and off-rate constant of the dye of 278 nM and 50/s, respectively. Ratios for Ca^{2+}-free (R_{min}) and Ca^{2+}-saturated (R_{max}) conditions were

4.0 and 0.7, respectively, based on calibrations. Most experiments were performed at room temperature (between 20°C and 25°C).

In voltage clamp experiments, we used a two-electrode system (SEC-05L-TEC; NPI-Electronic). The experiments were performed in an external solution (see Experimental solutions) providing conditions to eliminate all major ionic currents to ensure space clamping. Both intracellular electrodes were sharp micropipettes (ca. 7 MΩ) filled with 3 M KCl and were inserted close to each other near the center of the fiber. Rectangular voltage steps were applied from a holding potential of −80 mV.

Halothane application

To prepare halothane-air mixtures of defined concentrations, we used a vaporizer (Halothan-Vapor 19.3; Dräger) and measured the resulting halothane percentage with a calibrated infrared sensor (IRIS; Dräger). The anesthetic-containing gas mixture was equilibrated with Ringer's solution in a glass beaker that was part of a circular solution flow system. The halothane-containing Ringer's solution was passed at 2 ml/min through the experimental chamber on the microscope stage. The inlet to the chamber passed a custom-made electrical heating device that we used in some experiments to raise the temperature of the applied solution up to 35°C. Temperature was recorded with a miniature sensor positioned close to the cells under investigation.

We report concentration in percentage units (recorded with the calibrated IRIS system). In separate experiments, we took samples from the recording chamber and analyzed them using gas chromatography. The results confirmed that concentrations measured in the dish were proportional to readings from the IRIS systems with a conversion factor of 0.51 mM/%.

Data analysis

To estimate properties of Ca^{2+} removal and release during action potential–induced activation, we used an activation protocol consisting of a single pulse followed by several repetitive stimuli and a model to determine Ca^{2+} binding to major sites in the fiber as described (Braubach et al., 2014). Binding to Ca^{2+}-specific (T) sites and Ca^{2+}–Mg^{2+} (P) sites of troponin C was calculated as published (Robertson et al., 1981; Baylor and Hollingworth, 2003). The fixed rate constant and concentration values used for the calculations were as follows: for T-sites: $k_{on,T,Ca}$ = 115/µM/s, $k_{off,T,Ca}$ = 230/s; for P-sites: $k_{on,P,Ca}$ = 300/µM/s, $k_{off,P,Ca}$ = 0.6/s, $k_{on,P,Mg}$ = 0.1/µM/s, and $k_{off,P,Mg}$ = 2/s. $[T]_{tot}$ and $[P]_{tot}$, the total concentrations of T- and P-sites, were 240 µM each. $[Fura]_{tot}$ was 100 µM. Fast Ca^{2+} binding to ATP was described by a component proportional to free Ca^{2+} (scaling factor F = 3.6; Baylor and Hollingworth, 2003).

Any additional slow binding and slow Ca^{2+} sequestration (to the SR, mitochondria, etc.) was modeled using the combination of a saturable (S) and a nonsaturable (NS) first-order system whose constants ($[S]_{tot}$, $k_{on,S}$, $k_{off,S}$ and k_{NS}) were adjusted by least-squares-fitting the relaxation time courses as described in previous work (Melzer et al., 1986, 1987; Ursu et al., 2005; Braubach et al., 2014). Any model that provides a good simultaneous fit (for varying amounts of released Ca^{2+}) to the relaxation phases when release has stopped can be expected to describe overall removal of Ca^{2+} well and can be used to calculate Ca^{2+} release during the depolarizing stimuli. The Ca^{2+} removal model analysis was performed using software written in Delphi (Borland) and Visual Basics for Applications implemented in Excel (Microsoft; Ursu et al., 2005). Further analysis and statistical calculations were performed using the programming language R (R Core Team, 2014). Data in the text are presented as mean values ± SEM. Means of experimental group data were compared by two-sided unpaired t test, not assuming equal variances. Differences were considered significant when p-values were <0.05.

RESULTS

Halothane- and heat-induced Ca^{2+} elevation in YS compared with WT muscle fibers

In a first series of experiments, we superfused isolated muscle fibers of both WT and YS mice with Ringer's solution equilibrated with 3% halothane. Fig. 1 shows the averaged response of 14 WT and 20 YS fibers. Even though the WT cells showed a visible increase in free myoplasmic $[Ca^{2+}]$ on halothane application, the YS cells responded much more strongly. Mean free $[Ca^{2+}]$ values were significantly different at all measurement points.

Our experiments were generally performed at room temperature because the survival rate was very low when working with heated solutions, particularly in combination with the anesthetic drug. However, we explored the additional effect of temperature by heating up the inflowing solution to 35°C 10 min after the onset of halothane application, as demonstrated in Fig. 1 A. In each case, the temperature rise induced a further clear increase in the free myoplasmic $[Ca^{2+}]$.

Because washout using the circular perfusion system was relatively slow, we applied fresh, completely halothane-free solution from a separate channel of the perfusion system when the reversibility of halothane effects was tested. As can be seen in Fig. 1 A, reversibility was almost perfect in both WT and YS fibers challenged with halothane.

Removal analysis and Ca^{2+} release calculation

Action potentials are the physiological electrical signals causing Ca^{2+} release and contraction in muscle. Therefore, we were interested in determining whether action potential–induced Ca^{2+} release was changed in the sit-

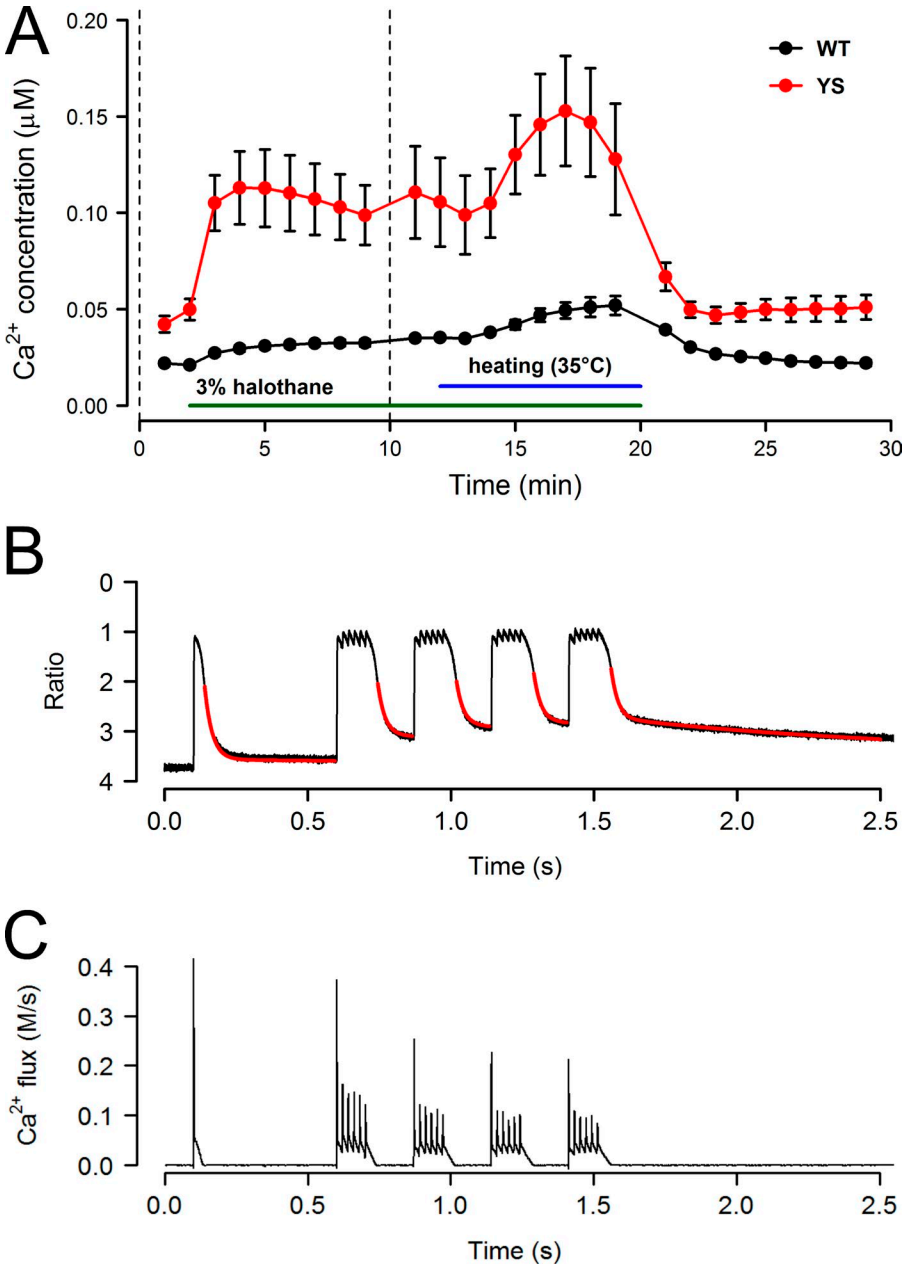

Figure 1. **Changes in Ca^{2+} concentration in response to halothane and temperature elevation.** [Ca^{2+}] was monitored in 1-min intervals over a period of 29 min. **(A)** Averaged data of 14 WT and 20 YS fibers. 3% Halothane was applied at minute 2. 10 min later, the temperature was raised from 25°C to 35°C. YS cells showed a significantly larger change than WT cells. The alterations were reversible. Error bars indicate SEM. **(B)** Representative example of Ca^{2+} removal model fitting (red lines) to a fura-2 fluorescence ratio trace resulting from repetitive field stimulation of action potentials in a WT fiber. **(C)** Ca^{2+} release flux derived from the measurement in B.

uations described in the preceding paragraph. All-or-none responsiveness was always tested at the start of the experiment, to ensure that the Ca^{2+} signals resulted from action potentials. To determine Ca^{2+} release, we applied a pulse protocol consisting of repetitive stimuli. A single pulse was followed by a silent period of 500 ms and four 50-Hz tetani, lasting 120 ms each, separated by 150-ms breaks (Fig. 1, B and C). The measurement contains five long relaxation intervals at different levels of released Ca^{2+} and therefore intracellular binding site saturation. It can be used to characterize Ca^{2+} removal. This pulse protocol was applied before and during the application of halothane (indicated by the dashed vertical lines in Fig. 1). We subjected the resulting fluorescence signals to an analysis generally known as removal model fitting (Melzer et al., 1986). In brief, the method we applied uses a Ca^{2+} binding and transport model and kinetic constants, partly available from the literature (see Materials and methods) and partly optimized by least squares fitting, to finally estimate the time course and extent of Ca^{2+} release (Braubach et al., 2014). The fit is performed in the relaxation phases of the repetitive fluorescence transients assuming that Ca^{2+} release has then ceased and the decay is exclusively caused by binding and transport. If this is not the case, part of the residual release activity would be attributed to slower removal and would consequently lower the estimated release, as we demonstrated by simulations (Timmer et al., 1998). Starting the model fitting early during relaxation of the fluorescence ratio signals produced only

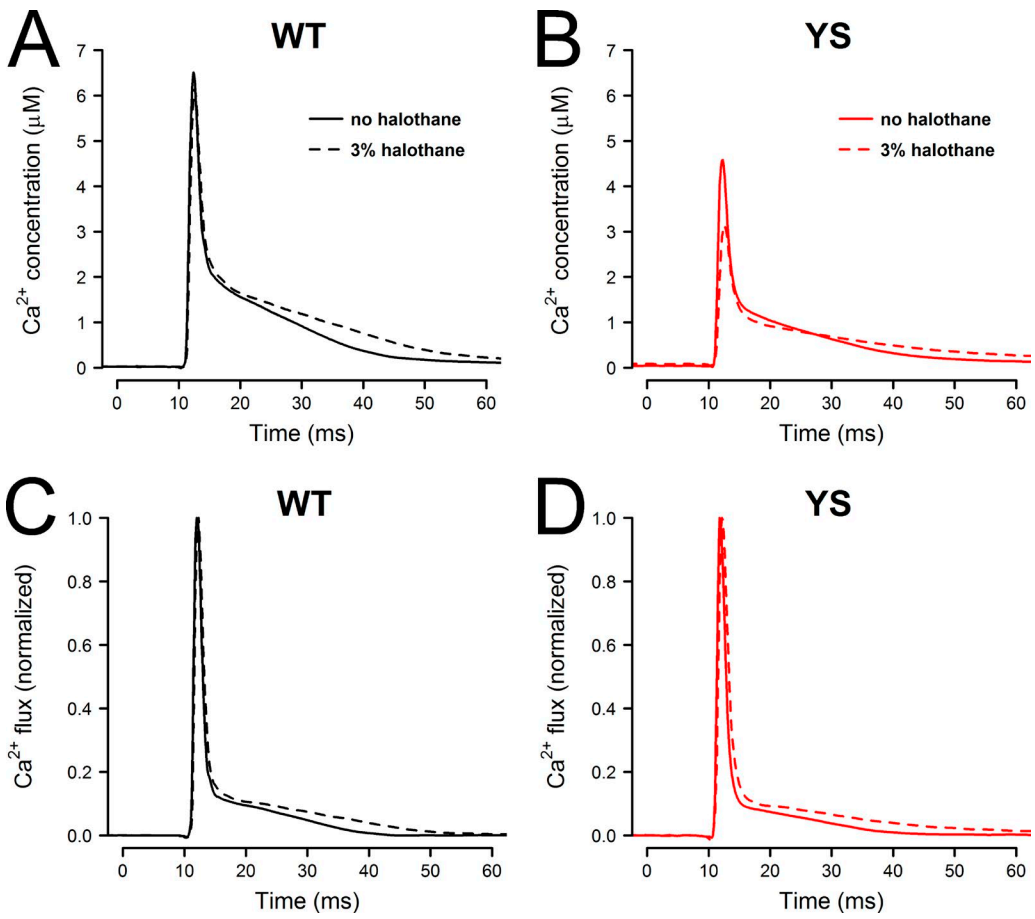

Figure 2. **Halothane slows the relaxation of action potential–induced Ca^{2+} transients.** Action potential–triggered Ca^{2+} signals were recorded at the instances indicated by the dashed vertical lines in Fig. 1 A. **(A and B)** Free Ca^{2+} transient before (continuous line) and after (dashed line) application of 3% halothane. **(C and D)** Ca^{2+} release flux (normalized to the peak) calculated from the data in A and B. The traces are averaged signals from 14 (WT) and 20 (YS) fibers, respectively. Mean best-fit parameters determined from the WT fibers in halothane-free solution and used for the calculations were as follows: $[S]_{tot}$ = (2.72 ± 0.30) mM, $k_{on,S}$, = (4.80 ± 0.61) · 10^6 $M^{-1}s^{-1}$, $k_{off,S}$ = (0.654 ± 0.020) s^{-1}, and k_{NS} = (1.20 ± 0.079) · 10^4 s^{-1}; n = 14.

small deviations between the measured fluorescence signal and the fitted curve in WT fibers, similar to previous results in another murine preparation (Braubach et al., 2014). In YS fibers and in the presence of halothane, the fit clearly deviated from the measurement. We consider this an indication of a component of extra release during relaxation. We therefore used the mean best-fit parameters (Fig. 2 legend) obtained in the 14 WT fibers with no halothane to calculate Ca^{2+} release flux from signals obtained with halothane and in mutant fibers. As an additional precaution, the fit in WT fibers was started later, when the fluorescence ratio signals had relaxed to approximately half their amplitude. The changes in $[Ca^{2+}]$ and Ca^{2+} release flux kinetics are summarized in Fig. 2. Shown are the averages (from different cells) of signals caused by the leading single pulse of the multipulse protocol (Fig. 1, B and C).

Fig. 2 (A and B) shows the free $[Ca^{2+}]$ transients, measured before (continuous lines) and during the halothane application (dashed lines). The WT transients (Fig. 2 A) exhibit the characteristics reported previously by others for type II fibers (Calderón et al., 2009). In particular, a fast and slow phase of relaxation is noticeable. Interestingly 3% halothane further delayed mainly the slow part, without significantly changing the mean peak of the signals. In YS fibers (Fig. 2 B), the mean amplitude of the transients was smaller and the relaxation phase slower than in WT fibers. Both amplitude and relaxation speed were further decreased by halothane.

Fig. 2 (C and D) shows the estimated Ca^{2+} release flux signals corresponding to the traces in Fig. 2 (A and B). To compare their time course, the signals were normalized to the peaks.

The result indicates a small residual component of release with delayed turnoff as the cause of the slow phase in free $[Ca^{2+}]$. Furthermore, it is the prolongation of this phase that seems to be the main cause of the alterations in relaxation speed of the $[Ca^{2+}]$ signals. The relaxation phases of both $[Ca^{2+}]$ transients and Ca^{2+} release flux signals were fitted using a dual exponen-

Table 1. **Kinetic effects of halothane on action potential–induced Ca^{2+} release**

Halothane (%)	τ_1 (ms)	P-value	A_2	P-value	τ_2 (ms)	P-value	Baseline	P-value	Peak	P-value	*n*
Free $[Ca^{2+}]$ (μM) WT											
0	0.552 ± 0.017		0.376 ± 0.012		15.58 ± 0.95		0.0203 ± 0.0016		6.74 ± 0.36		14
3	0.652 ± 0.041	0.0373[a]	0.371 ± 0.020	0.84	22.16 ± 1.80	0.00447[b]	0.0284 ± 0.0013	0.000548[c]	6.51 ± 0.40	0.673	13
Free $[Ca^{2+}]$ (μM) YS											
0	0.693 ± 0.029		0.327 ± 0.016		18.17 ± 1.14		0.0433 ± 0.0046		4.81 ± 0.24		20
3	0.916 ± 0.080	0.0162[a]	0.338 ± 0.016	0.6	32.30 ± 3.42	0.000881[c]	0.0834 ± 0.0144	0.0156[a]	3.32 ± 0.24	0.000103[c]	17
Ca^{2+} Flux (mM/s) WT											
0	0.649 ± 0.030		0.143 ± 0.012		12.71 ± 0.88		0.244 ± 0.019		343.71 ± 20.24		14
3	0.688 ± 0.030	0.363	0.153 ± 0.012	0.553	18.94 ± 1.65	0.00363[b]	0.340 ± 0.015	0.000548[c]	322.30 ± 17.29	0.429	13
Ca^{2+} Flux (mM/s) YS											
0	0.731 ± 0.030		0.115 ± 0.008		15.05 ± 1.34		0.519 ± 0.056		253.68 ± 13.01		20
3	0.855 ± 0.053	0.0526	0.119 ± 0.008	0.697	28.86 ± 3.86	0.003[b]	1.000 ± 0.172	0.0156[a]	163.76 ± 12.60	0.0000179[c]	17

The alterations in single action potential–induced responses demonstrated in Fig. 2 were quantified by nonlinear regression analysis. The relaxation phases of baseline-subtracted and peak-normalized free $[Ca^{2+}]$ and Ca^{2+} release flux traces were fitted by a dual exponential function: $f(t) = (1 - A_2) \cdot \exp[-(t - t_0)/\tau_1] + A_2 \cdot \exp[-(t - t_0)/\tau_2]$. The fit interval was 100 ms and started when traces had decreased by 5% of their peak value. Errors, SEM; *n*, number of experiments. P-values refer to changes caused by halothane.

[a]$P < 0.05$.

[b]$P < 0.01$.

[c]$P < 0.001$.

tial function (Table 1). Consistently, the time constant τ_2 (column 6) of the slow phase of relaxation was significantly increased (without a significant change of its fractional amplitude A_2; see column 4) when comparing measurements in halothane with those before halothane application. Columns 8 and 10 of Table 1 show means of the absolute values of free $[Ca^{2+}]$ and Ca^{2+} flux in the baseline and at the peak, respectively.

Small voltage changes strongly affect free myoplasmic $[Ca^{2+}]$ in YS fibers

The procedures described so far allowed investigation of the isolated fibers under close to physiological conditions (noninvasive Ca^{2+} recording, action potential activation of Ca^{2+} release). To pursue the question of whether and how the membrane potential modulates the effect of the anesthetic drug, we performed further experiments using the two-electrode voltage clamp technique, which allowed us to both stabilize the membrane at defined holding potentials during the drug application and apply differently depolarizing voltage steps to test for the ability of releasing Ca^{2+}. Unlike in our previous study of voltage-controlled Ca^{2+} release in YS muscle fibers (Andronache et al., 2009), we did not dialyze the cell but used sharp microelectrodes to minimally disturb the cytoplasm.

We subjected voltage-clamped fibers to a rigorous protocol that included the application of halothane and steady changes in the holding membrane potential, as demonstrated in Fig. 3. After impaling the microelectrodes and recording the basal Ca^{2+} level, the solution flow (2 ml/min) was started. The flow itself usually caused only very minor changes in free $[Ca^{2+}]$. 15 min after starting the perfusion, a steady depolarization to −70 mV was applied for 5 min, followed by a 10-mV hyperpolarization to −90 mV for another 5 min before the membrane voltage was set back to −80 mV. After another time interval of 10 min, the vaporizer system was turned on and adjusted such that the reading on the IRIS detector showed 0.2%. Ten minutes after starting the application of halothane, the same excursions of the membrane holding potential described before were applied. In the YS example (red) of Fig. 3, free $[Ca^{2+}]$ rose about fourfold shortly after applying halothane. After a partial decline, it started slowly rising again. When comparing the response to the depolarizing and hyperpolarizing voltage shifts, a dramatic difference to the no-halothane situation can be noticed. The small 10-mV depolarization caused a near doubling of the $[Ca^{2+}]$ level induced by halothane alone, and the hyperpolarization reduced the concentration markedly below this level. The black symbols in Fig. 3 show a typical example of applying the same protocol to a WT muscle fiber. Here, almost no change can be seen on superfusion with the halothane-containing solution, and the voltage responses are very small.

To quantify the voltage-induced Ca^{2+} signals, we fitted sloping lines to the three measurements before and after each voltage excursion. The line-subtracted free $[Ca^{2+}]$ changes were then analyzed to compare the voltage effects. Two series of experiments were performed, one with 0.2% halothane as shown in Fig. 3, and one with 0.5% halothane. The results of the individual measurements resembled the example shown. In Fig. 4, we pooled the results from the two se-

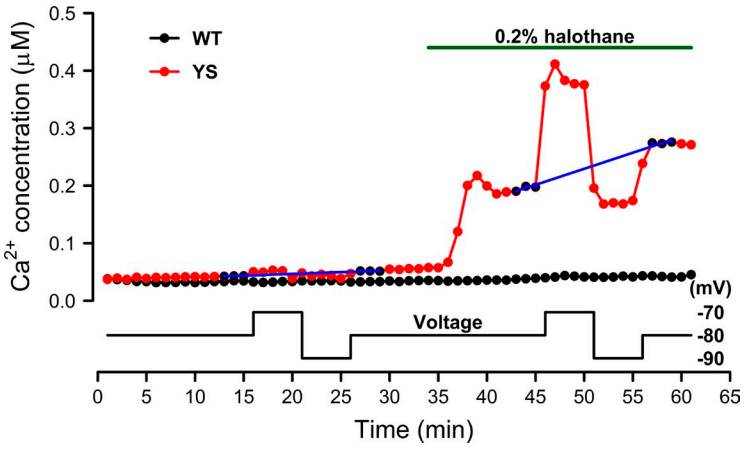

Figure 3. **Small voltage changes strongly modulate the halothane response in YS fibers.** Representative recordings in a WT and a YS fiber showing changes in free [Ca^{2+}] in response to a small concentration of halothane (0.2%) and small variations of the membrane potential in voltage-clamped fibers. A 10-mV depolarization and hyperpolarization (for 5 min each) from the holding potential of −80 mV was applied before and during the application of halothane. In the drug-free condition and in the WT fiber after halothane application, the voltage changes had little effect on the [Ca^{2+}] level. In contrast, the YS fiber responded strongly to halothane and to the subsequent small voltage alterations. The blue lines show linear fits to three recordings before and after the voltage changes. The lines were subtracted to determine the effect of the voltage change (see Fig. 4).

ries of experiments. The figure compares the holding potential–induced changes for halothane versus no halothane and demonstrates a highly significant difference in YS fibers, whereas WT fibers showed a very small difference.

Depolarizing pulses indicate altered voltage activation of Ca^{2+} release induced by halothane

The results presented in Figs. 3 and 4 clearly indicate that small changes in the resting potential can dramatically alter the effectiveness of halothane to stimulate Ca^{2+} release in YS muscle fibers. This result would be expected if there were a significant alteration in the voltage dependence of Ca^{2+} release caused by halothane in the way that the threshold for activation is shifted to more negative potentials. We pursued this possibility by combining the protocol of Fig. 3 with applying short voltage steps, depolarizing the membrane to different potentials before and after the application of halothane. To avoid excessive additional stress to the fibers, we applied only two pulses separated by a time interval of 1 s. The first one depolarized to −50 mV, which, in WT fibers, is close to but generally below the threshold of detection. The second one depolarized to −30 mV, which consistently leads to partial activation in WT fibers.

If the suspected voltage shift occurred, a rise in amplitude of the first response, relative to the second one, should be expected. Fig. 5, displaying mean free [Ca^{2+}] signals for WT and YS at 0, 0.2, and 0.5% halothane, shows that this is in fact the case. Because the mutation is known to shift the voltage dependence of activation as reported by us and others (Dietze et al., 2000; Ávila and Dirksen, 2001; Andronache et al., 2009), the smaller pulse was always above the threshold in YS in contrast to WT. When halothane was applied, the −50-mV depolarization caused a response in WT where there was none before. Moreover, in the YS fibers a strong potentiation of the −50-mV response relative to the −30-mV response can be noticed. A similar potentiation occurred in the WT fibers at 0.5% halothane. This indicates that halothane indeed caused a shift of the activation curve to more negative potentials in both cases. In contrast to WT fibers, the signals in the YS fibers declined in amplitude parallel to the rise in baseline [Ca^{2+}].

In Fig. 6, the Ca^{2+} signals of Fig. 5 are converted to estimates of Ca^{2+} release flux. For this, we used the mean model parameters obtained with the removal fit analysis from action potential–induced signals in WT fibers. In addition to the relative potentiation of the −50-mV response, these measurements indicate a remarkable slowing of the kinetics of release deactivation, compatible with the results from action potential–triggered signals (Fig. 2). Because the relaxation phases could not be fitted by two exponentials in these cases, we quantified the kinetic change by determining the half time of relaxation (Table 2). The mean half time in halothane-free solution was almost four times larger in YS compared with WT (24.4 vs. 6.5 ms) but reached similar values in 0.5% halothane (53.6 vs. 50.8 ms).

Fig. 7 uses the peak values of the mean flux signals shown in Fig. 6 for an approximate reconstruction of the alterations in voltage-dependent activation. For simplicity, the analysis assumes Boltzmann-type activation curves of equal steepness, with a constant steepness parameter k. We used k = 6.6 mV, which is close to the values determined for WT and YS in our previous study (Andronache et al., 2009). With this assumption, an approximate quantification of the alterations in fractional activation by halothane could be performed (Fig. 7). The procedure uses the fact that the ratio of the values at the two fixed voltages (given a canonical Boltzmann-type voltage dependence) shows a unique sigmoidal dependence on the voltage of half-maximal activation $V_{0.5}$ (Fig. 7 A). The filled circles in Fig. 7 A indicate the peak ratios of the measurements at the different conditions. Their abscissa values show the estimates of the $V_{0.5}$ values. This analysis predicts a shift in $V_{0.5}$ of −26.6 mV in WT (black) and −30.0 mV in YS (red) for 0.2% halothane. For the measurements with 0.5% halothane, the identical analysis leads to shifts in $V_{0.5}$ of

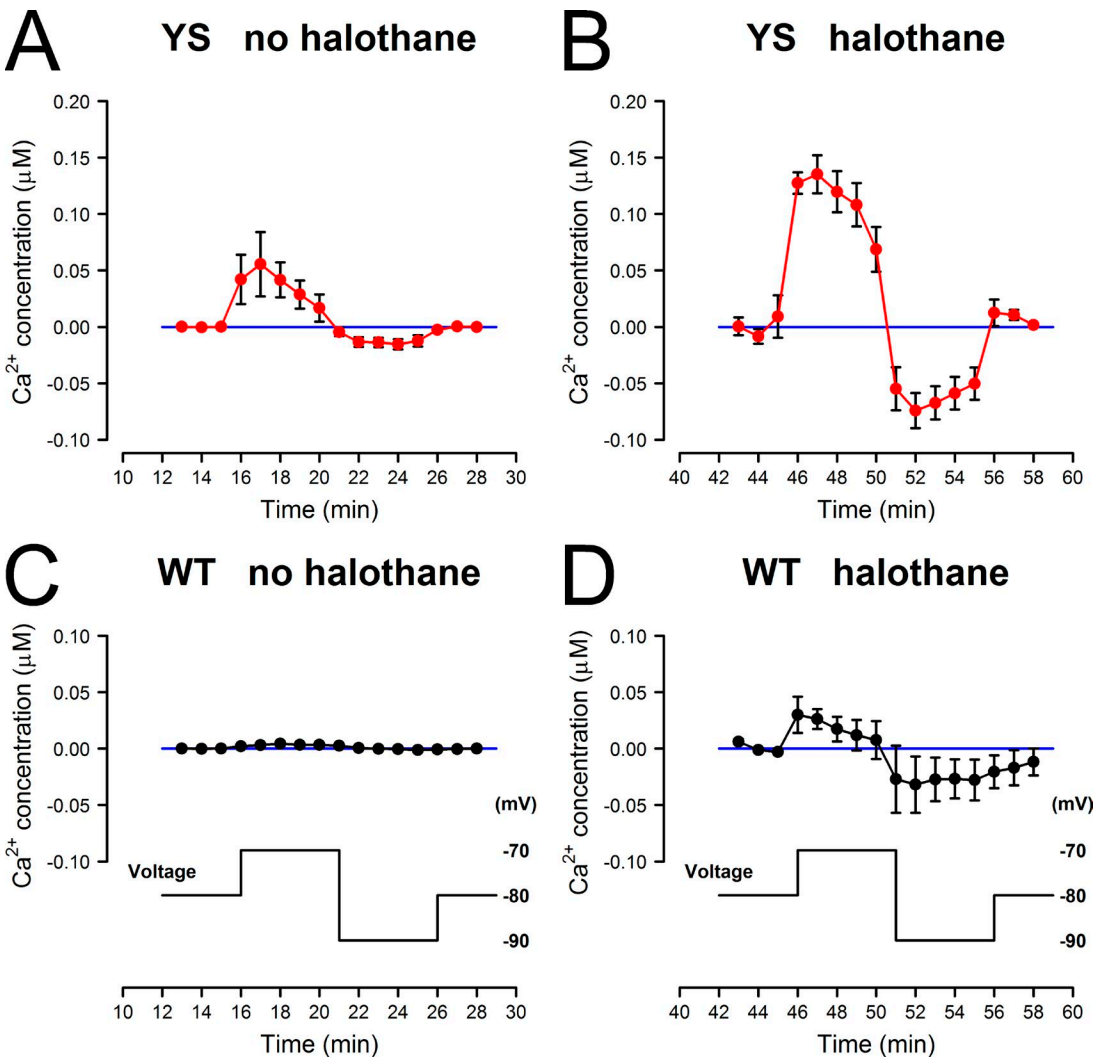

Figure 4. **Halothane alters the voltage sensitivity of the calcium level near the resting membrane potential.** Summarized results of experiments of the kind shown in Fig. 3. In each case, a sloping line was fitted to 3 min before and after the voltage change and subtracted (see blue lines in Fig. 3) to separate the response to voltage from the halothane-induced free [Ca^{2+}] level. Data with 0.2 and 0.5% of halothane were pooled. **(A and C)** YS and WT, respectively, before halothane application. **(B and D)** Same experiments during halothane application. Averaged data from 13 WT and 12 YS fibers. Error bars indicate SEM.

−34.1 mV for WT and 30.3 mV for YS. Fig. 7 B displays the fractional voltage dependencies derived from this analysis with the normalized flux amplitudes at the two test voltages included as filled circles.

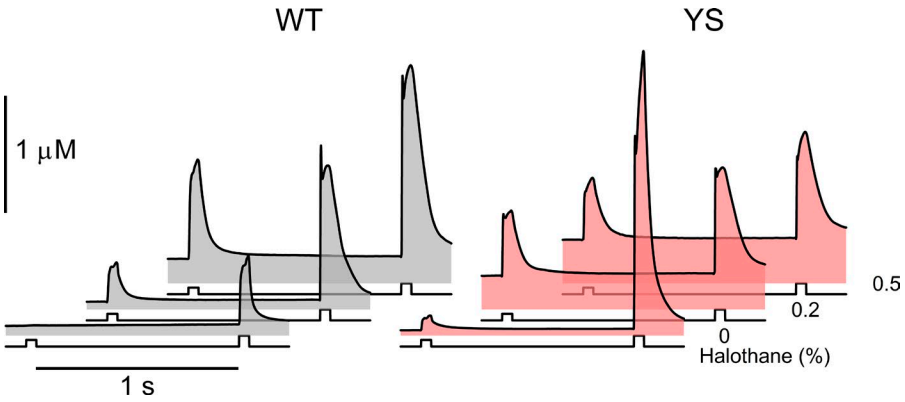

Figure 5. **Halothane alters the Ca^{2+} response to voltage pulse activation.** Averaged free [Ca^{2+}] traces of WT (gray shapes) and YS fibers (red shapes) demonstrating changes in baseline [Ca^{2+}] and the response to short (50-ms) depolarizations from a holding potential of −80 mV to −50 and −30 mV. Pulses are indicated underneath the traces and were separated by 1-s intervals. The effect of 0.2 and 0.5% halothane is shown.

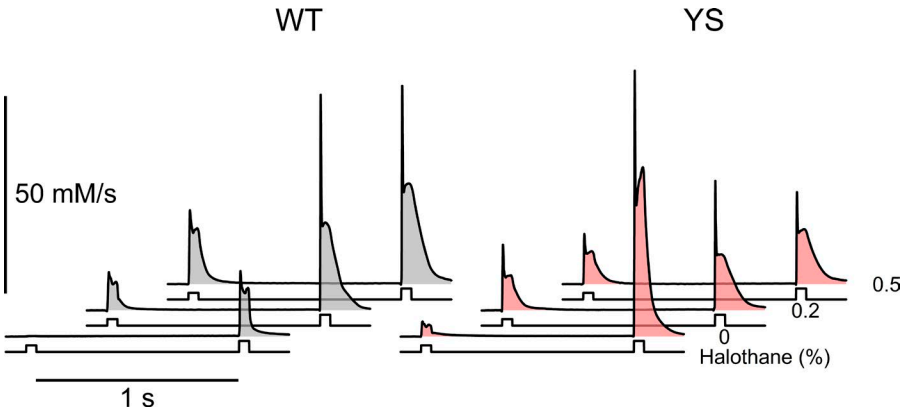

Figure 6. **Changes in depolarization-activated Ca^{2+} release flux caused by halothane.** Mean Ca^{2+} release flux traces from the same set of measurements as in Fig. 5. Note that halothane causes a decrease in the ratio of the respective pulse responses and a marked slowing in the deactivation of release. For quantitative comparison, see Table 2.

DISCUSSION

Skeletal muscle fiber depolarization is the trigger for rapid Ca^{2+} release during normal contractile performance. On the other hand, volatile anesthetics are potent chemical triggers of Ca^{2+} release in malignant hyperthermia-susceptible muscle. Here we investigated the cross relation between these two triggers in one of the available murine models of MH using halothane, an anesthetic trigger agent whose application is part of the standardized in vitro contracture test for MH susceptibility. We found that halothane lowers the threshold for voltage activation and that depolarization enhances the effectiveness of halothane.

Discriminating WT and YS fibers by their resting Ca^{2+} level and halothane response

Early fura-2 Ca^{2+} measurements in normal and MHS muscle cells of pigs and humans (Iaizzo et al., 1988, 1989b) showed altered caffeine and halothane responses but no significant difference in the resting free [Ca^{2+}] level, in contrast to measurements using Ca^{2+}-selective microelectrodes (Lopez et al., 1986). In the murine model used here, the initial mean resting [Ca^{2+}] in the experiments of Fig. 1 was significantly higher (P = 0.001) in the group of YS fibers compared with WT cells (42.2 ± 4.24 vs. 21.8 ± 1.43 μM). YS fibers could also be well distinguished from their WT counterparts by their much stronger response to halothane application. Nevertheless, WT fibers, too, showed an increase (even though much smaller) in resting [Ca^{2+}] when halothane was applied, consistent with the notion that the sensitivity to volatile anesthetics is inherent to the Ca^{2+} release system and not introduced by the MH mutation.

A drawback in our study is the fact that, for stability reasons, we had to perform our measurements at a temperature lower than physiological temperature. The single set of experiments in which we increased temperature on top of a preequilibration with 3% halothane (Fig. 1) demonstrates that halothane responses are enhanced at higher temperatures. Therefore, the results reported here will differ quantitatively but probably not qualitatively at higher temperatures.

Origin of kinetic alterations caused by mutation and halothane

Our method of converting the Ca^{2+} transients to Ca^{2+} release flux using the Ca^{2+} removal model approach shows that in YS fibers the overall amplitude of the flux is decreased considerably during halothane application and the slow phase of release is prolonged (Table 1). Given the elevated resting Ca^{2+} concentration, the decrease in amplitude likely results from a partial steady-state depletion of the SR leading to activation of store-operated Ca^{2+} entry. As has been reported by

Table 2. **Kinetic effects of halothane on Ca^{2+} release in voltage-clamped muscle fibers.**

Halothane (%)	WT					YS				
	$t_{0.5}$ (ms)	P-value	Ca^{2+} Flux (mM/s)	P-value	*n*	$t_{0.5}$ (ms)	*P*-value	Ca^{2+} Flux (mM/s)	P-value	*n*
0	6.46 ± 1.21		12.22 ± 3.00		12	24.42 ± 3.98		42.35 ± 4.47		13
0.2	49.3 ± 9.30	0.00951[a]	20.55 ±3.40	0.0949	5	58.0 ± 13.5	0.121	13.43 ± 1.47	0.0000272[b]	3
0.5	50.80 ± 4.81	0.000154[b]	25.07 ± 3.88	0.0238[c]	6	53.58 ± 9.17	0.0225[c]	13.64 ± 1.16	0.0000262[b]	6

Quantification of the relaxation time course of Ca^{2+} release after depolarization to −30 mV (the second response in the dual-pulse experiments of Fig. 6). The half time of relaxation was used for comparison. Ca^{2+} flux values were measured at the end of the depolarizing pulse. Errors, SEM; *n*, number of experiments. P-values refer to changes caused by halothane compared with measures before halothane application.

[a]P < 0.01.

[b]P < 0.001.

[c]P < 0.05.

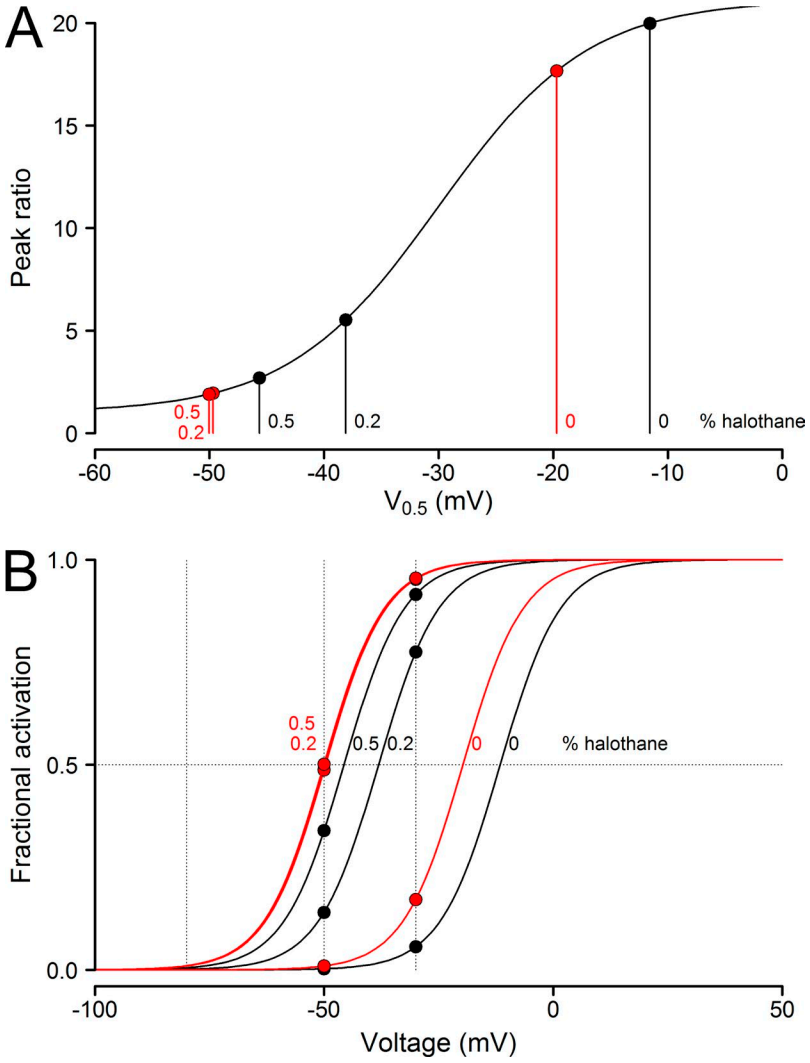

Figure 7. **Altered voltage dependence of Ca^{2+} release caused by halothane. (A)** Ratio between the activation at V_1 = −50 mV and V_2 = −30 mV assuming a standard Boltzmann-type activation curve [B(V)]: ratio($V_{0.5}$) = $B(V_2)/B(V_1)$ = {1 + exp[(V_1 − $V_{0.5}$)/k]}/{1 + exp[(V_2 − $V_{0.5}$)/k]}. The vertical lines point to the $V_{0.5}$ values estimated by iteratively solving the equation (−11.6, −38.1, and −45.6 mV for WT and −19.7, −49.7, and −50.0 mV for YS assuming a steepness parameter k = 6.6 mV). Black symbols, WT; red symbols, YS. Numbers indicate halothane percentage. **(B)** Activation as a function of voltage for the six different conditions shown in Fig. 6 derived from the analysis in A.

Manno et al. (2013), flexor digitorum brevis fibers of the YS mouse exhibit partial depletion already under nontriggering conditions.

Both action potential–triggered Ca^{2+} signals and voltage step-activated Ca^{2+} transients showed a consistently slower relaxation back to baseline. A change in relaxation kinetics, as observed here, can have several possible causes: (a) Ca^{2+} release could persist longer than normally even after repolarization, (b) the sequestration mechanisms (buffers with slow kinetics, Ca^{2+} transport mechanisms) could be less effective, and finally, (c) an increase in the cytoplasmic concentration of a fast equilibrating Ca^{2+} binding protein would decrease the amplitude and, consequently, slow down relaxation kinetics. The experiments could not unambiguously identify the reason for the slower relaxation. However, halothane has been demonstrated to favor Ca^{2+} permeation through isolated and reconstituted RyR1 channels (Nelson, 1992; Jiang et al., 2008). On the other hand, at low concentration, as used here, it has been shown to enhance the SR Ca^{2+} pump rather than inhibiting it (Karon et al., 1999). Also, it is difficult to see how halothane should mobilize a rapidly acting Ca^{2+} buffer. Therefore, we consider it most likely that the slower Ca^{2+} relaxation results from a slower turnoff of RyR1 permeation by repolarization, and the analysis was performed accordingly. It is interesting to note that the change in relaxation kinetics resembles the effect of low concentrations of caffeine in frog muscle fibers, which was attributed to a Ca^{2+}-induced component of Ca^{2+} release (Klein et al., 1990). Consistent with this explanation is the reported enhancement by volatile anesthetics of Ca^{2+}-induced Ca^{2+} release in skinned fibers (Matsui et al., 1991). Therefore, the prolongation can probably be attributed to the kinetic alteration of RyR1 gating induced by halothane. Although somewhat less pronounced, WT fibers, too, showed this effect, again in agreement with the view that sensitivity to halothane is inherently present and not introduced but strongly enhanced by the MH mutation.

Modulation of anesthetic strength by the membrane potential

In our voltage clamp experiments, we performed both long-lasting small changes in the holding potential and short-pulse depolarizations of larger amplitude. Together, these measurements showed that the application of halothane, even at relatively low concentrations, caused a very significant alteration in the activation voltage dependence of ECC. In WT muscle and YS muscle under drug-free conditions, the threshold for voltage activation is kept distant from the resting membrane potential, ensuring that fluctuations in the resting membrane potential will not immediately lead to Ca^{2+} stress. Relatively mild steady depolarizations have been shown to cause partial SR depletion even in WT fibers (Robin and Allard, 2013). In contrast, application of small concentrations of halothane shifts the threshold to more negative voltages than the normal resting values, with the consequence that even the normal resting potential will now lead to a substantial $[Ca^{2+}]$ elevation that cannot be compensated for by the intrinsic Ca^{2+} sequestration mechanisms.

One can also look at the situation from another point of view by considering the membrane potential as a strong modulator of the effectiveness of the drug in releasing Ca^{2+} from the SR. This is most evident from the results of Fig. 4. Unlike under drug-free conditions, the small alterations in the holding potential got translated to large changes in free myoplasmic $[Ca^{2+}]$ when halothane was present at low, clinically relevant concentrations. The result of Fig. 1 A suggests that these effects would be even larger at higher temperatures. Membrane depolarization likely occurs in heavily active muscle, for instance through the outward transfer of intracellular potassium ions (Allen et al., 2008), and heat development is a natural consequence of muscle metabolism. Therefore, it is easy to envisage that membrane depolarization together with warming and reactive oxidative chemical species can form an important part of the destructive feed-forward cycle (Durham et al., 2008) that has been suggested to lead into the fulminant MH crisis. Notably, Fig. 4 shows that hyperpolarization will have the opposite effect. Therefore, any intervention that hyperpolarizes or even only stabilizes the muscle membrane potential can be expected to have a beneficial effect in an MH crisis. A simple SR leak induced by the anesthetic drug in parallel to the ECC pathway of Ca^{2+} release would not show this effect. Despite the apparent partial loss of kinetic control, at least a large part of the leak remains under the command of the transverse tubular voltage sensor.

Similar conclusions can be drawn from previous experiments investigating potassium-conditioned caffeine contractures (Gallant et al., 1995). Caffeine is the second chemical tool (in addition to halothane) that is used in the IVCT diagnosis for MH susceptibility. A pre-depolarization to approximately −40 mV by 30 mM K^+ lowered the threshold for the caffeine response in muscle preparations of both normal and MHS pigs (Gallant et al., 1995). Therefore, the membrane potential may also be a source of variability in the diagnostic IVCT. This question has also been addressed in porcine and human biopsies by determining the effect of spontaneous depolarization on the contractile response (using halothane, caffeine, or both). The results vary, showing enhancement (Gallant et al., 1986), no effect (Iaizzo and Lehmann-Horn, 1989), and inhibition (Adnet et al., 1992) of the drug response. The reasons for this variability are not clear. They may originate from different conditions that caused the membrane to depolarize in the cited studies and a variable direct effect on Ca^{2+} release.

In addition to their effect on the RyR1 protein, anesthetics might have other channel targets in muscle (Franks, 2008) that could alter the membrane potential and boost the response. However, in MH-susceptible pigs, halothane contractures were not accompanied by fiber depolarization (Iaizzo et al., 1989a). Furthermore, elegant in vivo experiments by Eltit et al. (2013) on MH-susceptible mice, using Ca^{2+}-sensitive microelectrodes, measured $[Ca^{2+}]$ and membrane potential in parallel and demonstrated that the resting potential remained unchanged during anesthetic-induced $[Ca^{2+}]$ elevation.

Models to explain the findings

We discuss our results in terms of a primary modulation of the Ca^{2+} efflux from the SR. Basic principles require that any steady-state alteration of cytoplasmic free $[Ca^{2+}]$, as found here and in muscle fibers of another MH-susceptible mouse (Eltit et al., 2013), must have a contribution from Ca^{2+} entry from the extracellular space (Ríos, 2010). Thus, changing the holding potential might affect free cytoplasmic $[Ca^{2+}]$ also by directly driving a Ca^{2+} flux through voltage-independent pathways of the cell membrane. However, the alterations in free $[Ca^{2+}]$ that we observed when changing the holding potential (Figs. 3 and 4) are opposite to what one would expect if they arose simply from changing the driving force for Ca^{2+} entry through channels in the sarcolemma or the T-tubules. The changes are obviously linked to a voltage gating effect, very likely the DHPR-controlled EC coupling pathway.

That MH-susceptible muscle exhibits a higher sensitivity to membrane depolarization has first been reported by Gallant and Donaldson (1989) and Gallant and Lentz (1992) using potassium depolarization on mutant porcine muscle preparations. This effect has been confirmed by measuring Ca^{2+} signals in cultured and mature muscle cells by us and others (Dietze et al., 2000; Ávila and Dirksen, 2001; Andronache et al., 2009). We suggested a reaction scheme that appreciates the

allosteric conformational coupling between the DHPR and the RyR1 to explain the lower voltage threshold in MH-susceptible muscle. The model assumes a lowering of the energy of the open state of the RyR1 as the primary effect of the mutation. Because the RyR1 is mechanically coupled to the DHPR, the altered closed-open equilibrium of the RyR1 will "pull" at the voltage-dependent equilibrium between resting and active states of the DHPR and therefore favor the active state with the consequence of a displacement of the voltage activation curve to more negative potentials. The effect of an anesthetic drug on the EC coupling voltage dependence could be explained in a similar way if the drug binding further stabilizes the open conformation of the RyR1. In fact, this view is in line with current models of anesthetic action on neuronal targets. There it is thought that the drugs bind to specific conformations of the target channels, thus favoring functional states (Franks, 2008). If those conformations exhibit binding sites for physiological ligands, the ligand concentration dependence of channel activation will be altered in a similar way as the voltage dependence of Ca^{2+} release is altered in muscle.

In this scenario, the alteration in voltage dependence is a simple consequence of the coupled gating reactions of DHPR and RyR1. In addition, or alternatively, the coupling process itself might be changed as in the case of the chaotropic anion perchlorate. This substance likewise shifts the voltage dependence of activation (Gomolla et al., 1983; Lüttgau et al., 1983; González and Ríos, 1993; Csernoch et al., 1999) by affecting the ryanodine receptor (Ma et al., 1993; Anderson et al., 1997). However, it also increases the sensitivity of Ca^{2+} release to the voltage sensor input signal, reflected in an alteration of the "transfer function," i.e., the relationship between voltage sensor charge movement and Ca^{2+} release (González and Ríos, 1993; Ma et al., 1993; Ríos et al., 1993, 2015; Csernoch et al., 1999). Caffeine, too, left-shifts voltage-dependent activation (Lüttgau and Oetliker, 1968; Shirokova and Ríos, 1996a; Csernoch et al., 1999). A direct comparison of both drugs in mammalian muscle revealed differences in their transfer functions (Csernoch et al., 1999), indicating that they alter EC coupling in different ways. The effects of both caffeine and perchlorate have also been compared in WT versus MHS preparations by studying ryanodine receptor open probability and potassium-induced contractures (Anderson et al., 1997). The alterations in voltage dependence resembled our result of Fig. 7 with halothane. The available data suggest that, in the presence of these drugs, small shifts in holding potential would lead to similar responses as shown in our study for halothane (Fig. 3).

Another modulatory contributor to the halothane mechanism that should be considered is the $[Ca^{2+}]$ elevation itself. Enhancing effects of myoplasmic Ca^{2+} on the DHPR voltage sensing process have been demonstrated (Csernoch et al., 1991; González and Ríos, 1993; Shirokova and Ríos, 1996b). Furthermore, changes in the EC coupling transfer function and the DHPR-mediated L-type Ca^{2+} current have been attributed to the elevation in $[Ca^{2+}]$ (Feldmeyer et al., 1993; González and Ríos, 1993; Balog and Gallant, 1999). Investigations studying charge movements in relation to Ca^{2+} release and manipulating intracellular free $[Ca^{2+}]$ would be necessary to further analyze the mechanistic details by which membrane potential and anesthetic drugs interfere with each other in muscle.

Conclusion

In conclusion, we present clear evidence for the cross-influence of a volatile anesthetic drug and the membrane potential in a mature MH-susceptible muscle preparation. The results indicate a strong effect of the drug on the main characteristics of voltage-activated Ca^{2+} release and a sensitive modulation of the effectiveness of a given drug concentration by small variations of the membrane potential. These results can be explained by allosteric effects in the macromolecular complex constituting the calcium release units of the transverse tubular–SR junction. The detailed mechanisms and the consequences for diagnostics and therapeutics of these findings deserve further investigation.

ACKNOWLEDGMENTS

We are grateful to Dr. Susan L. Hamilton (Baylor College of Medicine, Houston, TX) for the gift of breeding pairs of Y524S mice and Dr. José R. López (Mount Sinai Medical Center, Miami Beach, FL) for information on the halothane application device. We thank Erhard Schoch (Institute of General Physiology, Ulm University) for valuable technical advice, Karin Fuchs (Institute of Applied Physiology, Ulm University) for expert technical help, and Michelle Bence for correcting the manuscript.

The authors declare no competing financial interests.

P. Elischer and M. Textor are recipients of a doctoral scholarship of the Medical Faculty of Ulm University. Deutsche Forschungsgemeinschaft research grant ME-713/18-2 to W. Melzer is gratefully acknowledged.

Author contributions: A. Zullo, acquisition of data, critical revision; M. Textor, acquisition of data, critical revision; P. Elischer, study conception, setup design; S. Mall, study conception, setup design; A. Alt, chemical analysis; W. Klingler, study conception, providing material; W. Melzer, study conception and design, analysis and interpretation of data, drafting of manuscript.

Eduardo Ríos served as editor.

Submitted: 29 July 2017
Accepted: 16 November 2017

REFERENCES

Adnet, P.J., R.M. Krivosic-Horber, M.M. Adamantidis, G. Haudecoeur, H.G. Reyford, and B.A. Dupuis. 1992. Is resting membrane potential a possible indicator of viability of muscle bundles used in the in vitro caffeine contracture test? *Anesth. Analg.* 74:105–111. https://doi.org/10.1213/00000539-199201000-00017

Allen, D.G., G.D. Lamb, and H. Westerblad. 2008. Skeletal muscle fatigue: Cellular mechanisms. *Physiol. Rev.* 88:287–332. https://doi.org/10.1152/physrev.00015.2007

Anderson, L.C., B.R. Fruen, R.C. Jordan, C.F. Louis, and E.M. Gallant. 1997. The action of perchlorate on malignant-hyperthermia-susceptible muscle. *Pflugers Arch.* 435:91–98. https://doi.org/10.1007/s004240050487

Andronache, Z., S.L. Hamilton, R.T. Dirksen, and W. Melzer. 2009. A retrograde signal from RyR1 alters DHP receptor inactivation and limits window Ca2+ release in muscle fibers of Y522S RyR1 knock-in mice. *Proc. Natl. Acad. Sci. USA.* 106:4531–4536. https://doi.org/10.1073/pnas.0812661106

Armstrong, C.M., F.M. Bezanilla, and P. Horowicz. 1972. Twitches in the presence of ethylene glycol bis(β-aminoethyl ether)-N,N′-tetracetic acid. *Biochim. Biophys. Acta.* 267:605–608. https://doi.org/10.1016/0005-2728(72)90194-6

Ávila, G., and R.T. Dirksen. 2001. Functional effects of central core disease mutations in the cytoplasmic region of the skeletal muscle ryanodine receptor. *J. Gen. Physiol.* 118:277–290. https://doi.org/10.1085/jgp.118.3.277

Balog, E.M., and E.M. Gallant. 1999. Modulation of the sarcolemmal L-type current by alteration in SR Ca2+ release. *Am. J. Physiol.* 276:C128–C135.

Baylor, S.M., and S. Hollingworth. 2003. Sarcoplasmic reticulum calcium release compared in slow-twitch and fast-twitch fibres of mouse muscle. *J. Physiol.* 551:125–138. https://doi.org/10.1113/jphysiol.2003.041608

Braubach, P., M. Orynbayev, Z. Andronache, T. Hering, G.B. Landwehrmeyer, K.S. Lindenberg, and W. Melzer. 2014. Altered Ca^{2+} signaling in skeletal muscle fibers of the R6/2 mouse, a model of Huntington's disease. *J. Gen. Physiol.* 144:393–413. https://doi.org/10.1085/jgp.201411255

Calderón, J.C., P. Bolaños, S.H. Torres, G. Rodríguez-Arroyo, and C. Caputo. 2009. Different fibre populations distinguished by their calcium transient characteristics in enzymatically dissociated murine flexor digitorum brevis and soleus muscles. *J. Muscle Res. Cell Motil.* 30:125–137. https://doi.org/10.1007/s10974-009-9181-1

Carroll, S.L., M.G. Klein, and M.F. Schneider. 1995. Calcium transients in intact rat skeletal muscle fibers in agarose gel. *Am. J. Physiol.* 269:C28–C34.

Chelu, M.G., S.A. Goonasekera, W.J. Durham, W. Tang, J.D. Lueck, J. Riehl, I.N. Pessah, P. Zhang, M.B. Bhattacharjee, R.T. Dirksen, and S.L. Hamilton. 2006. Heat- and anesthesia-induced malignant hyperthermia in an RyR1 knock-in mouse. *FASEB J.* 20:329–330.

Csernoch, L., G. Pizarro, I. Uribe, M. Rodríguez, and E. Ríos. 1991. Interfering with calcium release suppresses I γ, the "hump" component of intramembranous charge movement in skeletal muscle. *J. Gen. Physiol.* 97:845–884. https://doi.org/10.1085/jgp.97.5.845

Csernoch, L., P. Szentesi, and L. Kovács. 1999. Differential effects of caffeine and perchlorate on excitation-contraction coupling in mammalian skeletal muscle. *J. Physiol.* 520:217–230. https://doi.org/10.1111/j.1469-7793.1999.00217.x

Dayal, A., K. Schrötter, Y. Pan, K. Föhr, W. Melzer, and M. Grabner. 2017. The Ca2+ influx through the mammalian skeletal muscle dihydropyridine receptor is irrelevant for muscle performance. *Nat. Commun.* 8:475. https://doi.org/10.1038/s41467-017-00629-x

Dietze, B., J. Henke, H.M. Eichinger, F. Lehmann-Horn, and W. Melzer. 2000. Malignant hyperthermia mutation Arg615Cys in the porcine ryanodine receptor alters voltage dependence of Ca2+ release. *J. Physiol.* 526:507–514. https://doi.org/10.1111/j.1469-7793.2000.t01-1-00507.x

Durham, W.J., P. Aracena-Parks, C. Long, A.E. Rossi, S.A. Goonasekera, S. Boncompagni, D.L. Galvan, C.P. Gilman, M.R. Baker, N. Shirokova, et al. 2008. RyR1 S-nitrosylation underlies environmental heat stroke and sudden death in Y522S RyR1 knockin mice. *Cell.* 133:53–65. https://doi.org/10.1016/j.cell.2008.02.042

Eisner, D.A., J.L. Caldwell, K. Kistamás, and A.W. Trafford. 2017. Calcium and excitation-contraction coupling in the heart. *Circ. Res.* 121:181–195. https://doi.org/10.1161/CIRCRESAHA.117.310230

Eltit, J.M., X. Ding, I.N. Pessah, P.D. Allen, and J.R. Lopez. 2013. Nonspecific sarcolemmal cation channels are critical for the pathogenesis of malignant hyperthermia. *FASEB J.* 27:991–1000. https://doi.org/10.1096/fj.12-218354

Feldmeyer, D., W. Melzer, B. Pohl, and P. Zöllner. 1993. A possible role of sarcoplasmic Ca2+ release in modulating the slow Ca2+ current of skeletal muscle. *Pflugers Arch.* 425:54–61. https://doi.org/10.1007/BF00374503

Franks, N.P. 2008. General anaesthesia: From molecular targets to neuronal pathways of sleep and arousal. *Nat. Rev. Neurosci.* 9:370–386. https://doi.org/10.1038/nrn2372

Franzini-Armstrong, C., and F. Protasi. 1997. Ryanodine receptors of striated muscles: A complex channel capable of multiple interactions. *Physiol. Rev.* 77:699–729.

Gallant, E.M., and S.K. Donaldson. 1989. Skeletal muscle excitation-contraction coupling. II. Plasmalemma voltage control of intact bundle contractile properties in normal and malignant hyperthermic muscles. *Pflugers Arch.* 414:24–30. https://doi.org/10.1007/BF00585622

Gallant, E.M., and L.R. Lentz. 1992. Excitation-contraction coupling in pigs heterozygous for malignant hyperthermia. *Am. J. Physiol.* 262:C422–C426.

Gallant, E.M., T.F. Fletcher, V.M. Goettl, and W.E. Rempel. 1986. Porcine malignant hyperthermia: Cell injury enhances halothane sensitivity of biopsies. *Muscle Nerve.* 9:174–184. https://doi.org/10.1002/mus.880090211

Gallant, E.M., L.R. Lentz, and S.R. Taylor. 1995. Modulation of caffeine contractures in mammalian skeletal muscles by variation of extracellular potassium. *J. Cell. Physiol.* 165:254–260. https://doi.org/10.1002/jcp.1041650206

Gomolla, M., G. Gottschalk, and H.C. Lüttgau. 1983. Perchlorate-induced alterations in electrical and mechanical parameters of frog skeletal muscle fibres. *J. Physiol.* 343:197–214. https://doi.org/10.1113/jphysiol.1983.sp014888

González, A., and E. Ríos. 1993. Perchlorate enhances transmission in skeletal muscle excitation-contraction coupling. *J. Gen. Physiol.* 102:373–421. https://doi.org/10.1085/jgp.102.3.373

Guerrero-Hernández, A., G. Ávila, and A. Rueda. 2014. Ryanodine receptors as leak channels. *Eur. J. Pharmacol.* 739:26–38. https://doi.org/10.1016/j.ejphar.2013.11.016

Hernández-Ochoa, E.O., S.J. Pratt, R.M. Lovering, and M.F. Schneider. 2016. Critical role of intracellular RyR1 calcium release channels in skeletal muscle function and disease. *Front. Physiol.* 6:420. https://doi.org/10.3389/fphys.2015.00420

Hopkins, P.M. 2011. Malignant hyperthermia: Pharmacology of triggering. *Br. J. Anaesth.* 107:48–56. https://doi.org/10.1093/bja/aer132

Hopkins, P.M., H. Rüffert, M.M. Snoeck, T. Girard, K.P.E. Glahn, F.R. Ellis, C.R. Müller, and A. Urwyler. European Malignant Hyperthermia Group. 2015. European Malignant Hyperthermia Group guidelines for investigation of malignant hyperthermia susceptibility. *Br. J. Anaesth.* 115:531–539. https://doi.org/10.1093/bja/aev225

Hwang, J.H., F. Zorzato, N.F. Clarke, and S. Treves. 2012. Mapping domains and mutations on the skeletal muscle ryanodine

receptor channel. *Trends Mol. Med.* 18:644–657. https://doi.org/10.1016/j.molmed.2012.09.006

Iaizzo, P.A., and F. Lehmann-Horn. 1989. The in vitro determination of susceptibility to malignant hyperthermia. *Muscle Nerve.* 12:184–190. https://doi.org/10.1002/mus.880120304

Iaizzo, P.A., W. Klein, and F. Lehmann-Horn. 1988. Fura-2 detected myoplasmic calcium and its correlation with contracture force in skeletal muscle from normal and malignant hyperthermia susceptible pigs. *Pflugers Arch.* 411:648–653. https://doi.org/10.1007/BF00580861

Iaizzo, P.A., F. Lehmann-Horn, S.R. Taylor, and E.M. Gallant. 1989a. Malignant hyperthermia: Effects of halothane on the surface membrane. *Muscle Nerve.* 12:178–183. https://doi.org/10.1002/mus.880120303

Iaizzo, P.A., M. Seewald, S.G. Oakes, and F. Lehmann-Horn. 1989b. The use of Fura-2 to estimate myoplasmic [Ca2+] in human skeletal muscle. *Cell Calcium.* 10:151–158. https://doi.org/10.1016/0143-4160(89)90069-9

Jiang, D., W. Chen, J. Xiao, R. Wang, H. Kong, P.P. Jones, L. Zhang, B. Fruen, and S.R.W. Chen. 2008. Reduced threshold for luminal Ca2+ activation of RyR1 underlies a causal mechanism of porcine malignant hyperthermia. *J. Biol. Chem.* 283:20813–20820. https://doi.org/10.1074/jbc.M801944200

Karon, B.S., J.M. Autry, Y. Shi, C.E. Garnett, G. Inesi, L.R. Jones, H. Kutchai, and D.D. Thomas. 1999. Different anesthetic sensitivities of skeletal and cardiac isoforms of the Ca-ATPase. *Biochemistry.* 38:9301–9307. https://doi.org/10.1021/bi990190u

Klein, M.G., B.J. Simon, and M.F. Schneider. 1990. Effects of caffeine on calcium release from the sarcoplasmic reticulum in frog skeletal muscle fibres. *J. Physiol.* 425:599–626. https://doi.org/10.1113/jphysiol.1990.sp018120

Lanner, J.T., D.K. Georgiou, A.D. Joshi, and S.L. Hamilton. 2010. Ryanodine receptors: Structure, expression, molecular details, and function in calcium release. *Cold Spring Harb. Perspect. Biol.* 2:a003996. https://doi.org/10.1101/cshperspect.a003996

Larach, M.G. 1989. Standardization of the caffeine halothane muscle contracture test. North American Malignant Hyperthermia Group. *Anesth. Analg.* 69:511–515. https://doi.org/10.1213/00000539-198910000-00015

Liu, Y., E.G. Kranias, and M.F. Schneider. 1997. Regulation of Ca2+ handling by phosphorylation status in mouse fast- and slow-twitch skeletal muscle fibers. *Am. J. Physiol.* 273:C1915–C1924.

Lopez, J.R., L.A. Alamo, D.E. Jones, L. Papp, P.D. Allen, J. Gergely, and F.A. Sréter. 1986. [Ca2+]i in muscles of malignant hyperthermia susceptible pigs determined in vivo with Ca2+ selective microelectrodes. *Muscle Nerve.* 9:85–86.

Lüttgau, H.C., and H. Oetliker. 1968. The action of caffeine on the activation of the contractile mechanism in straited muscle fibres. *J. Physiol.* 194:51–74. https://doi.org/10.1113/jphysiol.1968.sp008394

Lüttgau, H.C., G. Gottschalk, L. Kovács, and M. Fuxreiter. 1983. How perchlorate improves excitation-contraction coupling in skeletal muscle fibers. *Biophys. J.* 43:247–249. https://doi.org/10.1016/S0006-3495(83)84346-X

Ma, J., K. Anderson, R. Shirokov, R. Levis, A. González, M. Karhanek, M.M. Hosey, G. Meissner, and E. Ríos. 1993. Effects of perchlorate on the molecules of excitation-contraction coupling of skeletal and cardiac muscle. *J. Gen. Physiol.* 102:423–448. https://doi.org/10.1085/jgp.102.3.423

Manno, C., L. Figueroa, L. Royer, S. Pouvreau, C.S. Lee, P. Volpe, A. Nori, J. Zhou, G. Meissner, S.L. Hamilton, and E. Ríos. 2013. Altered Ca2+ concentration, permeability and buffering in the myofibre Ca2+ store of a mouse model of malignant hyperthermia. *J. Physiol.* 591:4439–4457. https://doi.org/10.1113/jphysiol.2013.259572

Matsui, K., Y. Fujioka, H. Kikuchi, O. Yuge, K. Fujii, M. Morio, and M. Endo. 1991. Effects of several volatile anesthetics on the Ca(2+)-related functions of skinned skeletal muscle fibers from the guinea pig. *Hiroshima J. Med. Sci.* 40:9–13.

Melzer, W., E. Ríos, and M.F. Schneider. 1986. The removal of myoplasmic free calcium following calcium release in frog skeletal muscle. *J. Physiol.* 372:261–292. https://doi.org/10.1113/jphysiol.1986.sp016008

Melzer, W., E. Rios, and M.F. Schneider. 1987. A general procedure for determining the rate of calcium release from the sarcoplasmic reticulum in skeletal muscle fibers. *Biophys. J.* 51:849–863. https://doi.org/10.1016/S0006-3495(87)83413-6

Melzer, W., A. Herrmann-Frank, and H.C. Lüttgau. 1995. The role of Ca2+ ions in excitation-contraction coupling of skeletal muscle fibres. *Biochim. Biophys. Acta.* 1241:59–116. https://doi.org/10.1016/0304-4157(94)00014-5

Nelson, T.E. 1992. Halothane effects on human malignant hyperthermia skeletal muscle single calcium-release channels in planar lipid bilayers. *Anesthesiology.* 76:588–595. https://doi.org/10.1097/00000542-199204000-00016

R Core Team. 2014 R: A Language and Environment for Statistical Computing. Available at: http://www.R-project.org/

Ríos, E. 2010. The cell boundary theorem: A simple law of the control of cytosolic calcium concentration. *J. Physiol. Sci.* 60:81–84. https://doi.org/10.1007/s12576-009-0069-z

Ríos, E., M. Karhanek, J. Ma, and A. González. 1993. An allosteric model of the molecular interactions of excitation-contraction coupling in skeletal muscle. *J. Gen. Physiol.* 102:449–481. https://doi.org/10.1085/jgp.102.3.449

Ríos, E., L. Figueroa, C. Manno, N. Kraeva, and S. Riazi. 2015. The couplonopathies: A comparative approach to a class of diseases of skeletal and cardiac muscle. *J. Gen. Physiol.* 145:459–474. https://doi.org/10.1085/jgp.201411321

Robertson, S.P., J.D. Johnson, and J.D. Potter. 1981. The time-course of Ca2+ exchange with calmodulin, troponin, parvalbumin, and myosin in response to transient increases in Ca2+. *Biophys. J.* 34:559–569. https://doi.org/10.1016/S0006-3495(81)84868-0

Robin, G., and B. Allard. 2013. Major contribution of sarcoplasmic reticulum Ca^{2+} depletion during long-lasting activation of skeletal muscle. *J. Gen. Physiol.* 141:557–565. https://doi.org/10.1085/jgp.201310957

Rosenberg, H., J.F. Antognini, and S. Muldoon. 2002. Testing for malignant hyperthermia. *Anesthesiology.* 96:232–237. https://doi.org/10.1097/00000542-200201000-00036

Rosenberg, H., N. Pollock, A. Schiemann, T. Bulger, and K. Stowell. 2015. Malignant hyperthermia: A review. *Orphanet J. Rare Dis.* 10:93. https://doi.org/10.1186/s13023-015-0310-1

Shirokova, N., and E. Ríos. 1996a. Activation of Ca2+ release by caffeine and voltage in frog skeletal muscle. *J. Physiol.* 493:317–339. https://doi.org/10.1113/jphysiol.1996.sp021386

Shirokova, N., and E. Ríos. 1996b. Caffeine enhances intramembranous charge movement in frog skeletal muscle by increasing cytoplasmic Ca2+ concentration. *J. Physiol.* 493:341–356. https://doi.org/10.1113/jphysiol.1996.sp021387

Spiecker, W., W. Melzer, and H.C. Lüttgau. 1979. Extracellular Ca2+ and excitation-contraction coupling. *Nature.* 280:158–160. https://doi.org/10.1038/280158a0

Timmer, J., T. Müller, and W. Melzer. 1998. Numerical methods to determine calcium release flux from calcium transients in muscle cells. *Biophys. J.* 74:1694–1707. https://doi.org/10.1016/S0006-3495(98)77881-6

Ursu, D., R.P. Schuhmeier, and W. Melzer. 2005. Voltage-controlled Ca2+ release and entry flux in isolated adult muscle fibres of the mouse. *J. Physiol.* 562:347–365. https://doi.org/10.1113/jphysiol.2004.073882

Van Petegem, F. 2015. Ryanodine receptors: Allosteric ion channel giants. *J. Mol. Biol.* 427:31–53. https://doi.org/10.1016/j.jmb.2014.08.004

Yang, T., J. Riehl, E. Esteve, K.I. Matthaei, S. Goth, P.D. Allen, I.N. Pessah, and J.R. Lopez. 2006. Pharmacologic and functional characterization of malignant hyperthermia in the R163C RyR1 knock-in mouse. *Anesthesiology.* 105:1164–1175. https://doi.org/10.1097/00000542-200612000-00016